Toward GHz-Photodetection with Transition Metal Dichalcogenides

Fabian Straußˈ[1,2], Zhouxiaosong Zeng[1], Kai Braun,[1,2], Marcus Scheeleˈ[,1,2]*

[1] Institute of Physical and Theoretical Chemistry, Universität Tübingen, Auf der Morgenstelle 18, D-72076 Tübingen, Germany

[2] Center for Light-Matter Interaction, Sensors & Analytics LISA+, Universität Tübingen, Auf der Morgenstelle 15, D-72076 Tübingen, Germany

KEYWORDS Transition metal dichalcogenides, photodetectors, two-dimensional materials

CONSPECTUS

Transition metal dichalcogenides (TMDCs) exhibit favorable properties for optical communication in the GHz regime, such as large mobilities, high extinction coefficients and silicon compatibility. While impressive improvements of their sensitivity have been realized, the bandwidths of these devices have been mostly limited to few MHz. We argue that this shortcoming originates in the relatively large RC constants of TMDC-based photodetectors, which suffer from high surface defect densities, inefficient charge carrier injection at the electrode/TMDC interface and long charging times. However, we show in a series of papers that rather simple adjustments in the device architecture afford TMDC-based photodetectors with bandwidths of several 100s MHz.

We rationalize the success of these adjustments in terms of the specific physical-chemical properties of TMDCs, namely their anisotropic in-plane/out-of-plane carrier behavior, large optical absorption, and chalcogenide-dependent surface chemistry. Just one surprisingly simple yet effective pathway to fast TMDC photodetection is the reduction of the photoresistance by using light-focusing optics, which enables bandwidths of 0.23 GHz with an energy consumption of only 27 fJ/bit.

By reflecting on the ultrafast intrinsic photoresponse times of few picoseconds in TMDC heterostructures, we motivate the application of more demanding chemical strategies to exploit such ultrafast intrinsic properties for true GHz-operation in real devices. A key aspect in this regard is the management of surface defects, which we discuss in terms of its dependence on the layer thickness, its tunability by molecular adlayers and the prospects of replacing thermally evaporated metal contacts by laser-printed electrodes fabricated with inks of metalloid clusters. We highlight the benefits of combining TMDCs with graphene to heterostructures that exhibit the ultrafast photoresponse and large spectral range of Dirac materials with the low dark current and high responsivities of semiconductors. We introduce the bulk photovoltaic effect in TMDC-based materials with broken inversion symmetry as well as a combination of TMDCs with plasmonic nanostructures as means for increasing the bandwidth and responsivity simultaneously. Finally, we describe the prospects of embedding TMDC photodetectors into optical cavities with the objective of tuning the lifetime of the photoexcited state and increasing the carrier mobility in the photoactive layer.

The findings and concepts detailed in this account demonstrate that GHz photodetection with TMDCs is feasible, and we hope that these bright prospects for their application as next-generation

optoelectronic material motivates more chemists and material scientists to actively pursue the development of the more complicated material combinations outlined here.

KEY REFERENCES

1) Strauß, F.; Kohlschreiber, P.; Keck, J.; Michel, P.; Hiller, J.; Meixner, A. J.; Scheele, M. A simple 230 MHz Photodetector Based on Exfoliated WSe_2 Multilayers. *ChemRxiv Preprint* **2023**. https://doi.org/10.26434/chemrxiv-2023-0lmgq.[1] *The influence of the photoresistance onto the response speed of WSe_2 photodetectors is shown and lowered by using focusing optics to result in a bandwidth > 230 MHz.*

2) Strauß, F.; Schedel, C.; Scheele, M. Edge Contacts accelerate the Response of MoS_2 Photodetectors. *Nanoscale Advances* **2023**, 5, 3494. http://doi.org/10.1039/d3na00223c.[2] *For the first time edge contacts are examined towards their influence on the response speed of TMDC photodetectors.*

3) Schedel, C.; Strauß, F.; Kohlschreiber, P.; Geladari, O.; Meixner, A. J.; Scheele, M. Substrate Effects on the Speed Limiting Factor of WSe_2 Photodetectors. *Phys. Chem. Chem. Phys.* **2022**, 24, 25383 - 25390. https://doi.org/10.1039/D2CP03364J.[3] *Polyimide and glass are used to show the influence of substrates with different dielectric constants on the speed limiting mechanism in WSe_2 photodetectors.*

4) Maier, A.; Strauß, F.; Kohlschreiber, P.; Schedel, C.; Braun, K.; Scheele, M. Sub-nanosecond Intrinsic Response Time of PbS Nanocrystal IR-Photodetectors. *Nano Lett*. **2022**, 22, 2809-2816. https://doi.org/10.1021/acs.nanolett.1c04938.[4] *Asynchronous Optical Sampling is*

introduced for measuring the intrinsic response time of photoactive materials, and its application is exemplified for PbS nanocrystal photodetectors.

Introduction

Transition metal dichalcogenides (TMDCs), especially two-dimensional monolayers, exhibit strong excitonic binding energies (300 meV), large carrier mobilities (30 cm^2/Vs) and high extinction coefficients (~$3*10^6$ cm^{-1}).[5–7] They are chemically versatile, compatible with silicon technology, relatively cheap, and can be used as monolayers, multilayers or combined with other 2D materials in heterostructures. These properties are ideal for their application in photodetectors with high speed and large detectivity at the same time. However, as detailed by Sorger et al.[8] an independent optimization of speed and detectivity (or responsivity) is not possible, since the long carrier lifetimes needed for high responsivities are detrimental for the response time. Similarly, large mobilities are required for fast photodetection with sufficiently large band gaps to prevent high dark currents and, thus, low detectivities as e.g. in zero-gap graphene. Over the past ten years, most efforts have focused with impressive results on increasing the responsivity.[9] In contrast, similar improvements of the response speed of TMDC photodetectors have been challenging, and in particular a GHz photoresponse has remained mostly elusive, despite an increasing demand for GHz-compatible photodetectors as components in optical data communication. In this account, we reflect on the lessons learnt from our own physical-chemical approaches toward ultrafast TMDCs photodetectors.

The article is structured as follows: We begin with a brief account of the fundamental performance parameters of photodetectors for readers new to the field (see Box 1). We continue with a definition and distinction of extrinsic vs. intrinsic response times, discuss the effect of the TMDC layer thickness and provide a brief overview of the speed limiting factors in TMDC

photodetectors. On this basis, we devise chemical and physical design strategies for accelerating their photoresponse, taking into account substrate considerations, chemical healing of defects, edge electrodes and reducing the photoresistance. We conclude with promising future directions to even faster photodetection, including optical cavities, the bulk photovoltaic effect and plasmonics.

Box 1: Figures of merit of photodetectors[10,11]

Selection of sensitivity measures:

Responsivity $\Re = \frac{I_{Photo}}{P_{Laser}}$

Switching energy $E_{switch} = \frac{P_{Laser}}{BW}$

Detectivity $D = \frac{\Re\sqrt{A}}{\sqrt{2*qI_{dark}}}$

ON/OFF ratio $\frac{ON}{OFF} = \frac{I_{ON}}{I_{OFF}}$

Rise and fall time in the non-steady and steady state:

The time it takes the current to increase from 10 to 90% (90 to 10%) of its final value is called the rise (fall) time. Two different laser excitations are distinguished: Steady (a) and non-steady state (b) excitation, as sketched below. In the steady state a square pulse illumination increases the current to the highest possible photocurrent. The non-steady state mimics real data transfer by illumination with a delta shaped impulse and observing the response time. Via the power spectrum, the frequency-based speed measure, the 3dB bandwidth, can be determined, giving the maximal operation frequency at which the initial photocurrent has dropped to 70%.[12] Note that the often-used approximation $t_{rise} = 0.35/f_{3dB}$ can lead to large deviations compared to the much more precise power spectrum, when calculating the bandwidth.[13]

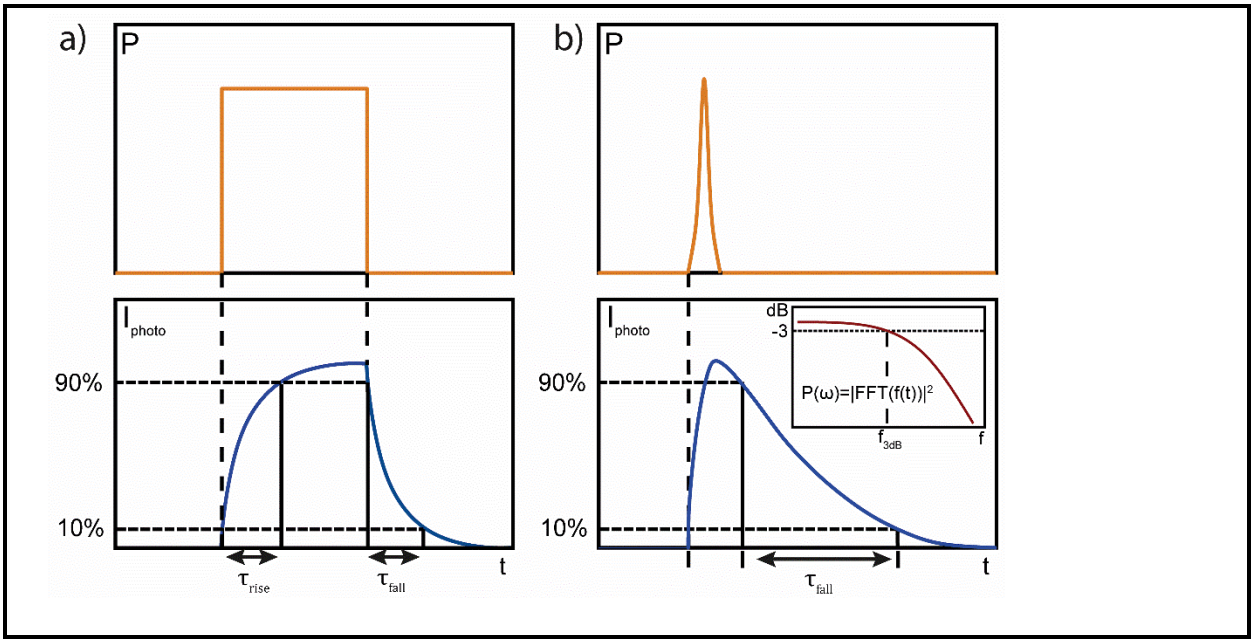

Extrinsic vs. intrinsic response

The *extrinsic* photoresponse is the true signal processing time (detector speed) of the entire device with highest relevance for real applications. The basic concepts for its experimental determination are detailed in Box 1. A laser with a pulse length much shorter than the response time excites the photoactive material to assess the rise and fall times, limited by the slowest mechanism present. Possible limitations are the RC time, drift / transit time and diffusion time.[14] The RC time t_{RC} is the product of the device capacitance and the device resistance, which is omnipresent in every electrical component. The transit time depends on the mobility μ, the channel length d and the applied bias U: $t_{transit} = \frac{d^2}{\mu * U}$. Diffusion is only important in non-depleted regions, depending on the diffusion length l and the diffusion coefficient D: $t_{diff} = \frac{l^2}{D}$. By increasing the depletion region or the material mobility, the diffusion zones get smaller, and the slow diffusion component vanishes.

These mechanisms are expressed as $t_{rise} = \sqrt{t_{diff}^2 + t_{drift}^2 + (2.2 * \tau_{RC})^2}$, since the RC time must be multiplied with 2.2 to account for the 10 – 90% niveau. Further, more specific effects

included in these fundamental three components are the carrier injection time at the electrode and the transfer time between two materials in a heterostructure or even between two layers in a multilayer. The injection time or electrode-material transfer time is found indirectly in the RC time in form of the contact resistance whereas the material-transfer time is part of the drift or diffusion time, depending on the depletion.

In contrast, the *intrinsic* response time reflects the inherent lifetime circle of charge carriers from exciton dissociation to photocurrent generation. Therefore, the intrinsic response time constitutes the upper limit to the speed of a photodetector if all external factors (e.g. RC time) are negligible. Its determination requires all-optical methods, such as the two-pulse coincidence (2PC) technique, which is detailed in Box 2. Briefly, a pulsed pump laser excites the sample and after a short delay, a second laser, the probe laser, examines how many charge carriers can be re-excited. The temporal resolution of this experiment is given by the pulse width of the pump laser and/or the delay time between the two lasers, such that measurements with dt < 100 fs are possible.

For the entire charge carrier lifetime, the intrinsic response time τ_{in} can be expressed as follows: $\tau_{in}^{-1} = (\tau_d + \tau_s)^{-1} + \tau_r^{-1}$,

where τ_d is the charge carrier drift time, τ_s the charge carrier transfer time e.g. between two TMDCs, and τ_r the charge carrier recombination time. More details on different recombination processes can be seen in Box 2. Typical values of τ_{in} vary from several picoseconds to hundreds of nanoseconds.[15]

Box 2: Scheme of two-pulse coincidence (2PC) photoresponse measurements

At a small pump-probe delay, due to the saturated absorption of the charge carriers in the ground state of the active material, the photocurrent generated by the second pulse will be suppressed. With the increase in delay time, parts of the excited charged carriers return to the

ground state and can be excited again, therefore the generated photocurrent demonstrates an exponential recovery, reflecting the intrinsic response time of a photodetector, see Figure a-d below.

The working principle of asynchronous optical sampling (ASOPS) is similar, however, a detuning repetition frequency Δf of the pump laser compared to the probe laser is adopted to form a pump-probe delay. With the repetition frequency difference Δf, when the first pulses of the pump laser and the probe laser coincide, a successive offset for the subsequent pulses as a delay time will be generated. Delay times range from femtoseconds to several ns (5 ns for 100 MHz repetition rate).[4]

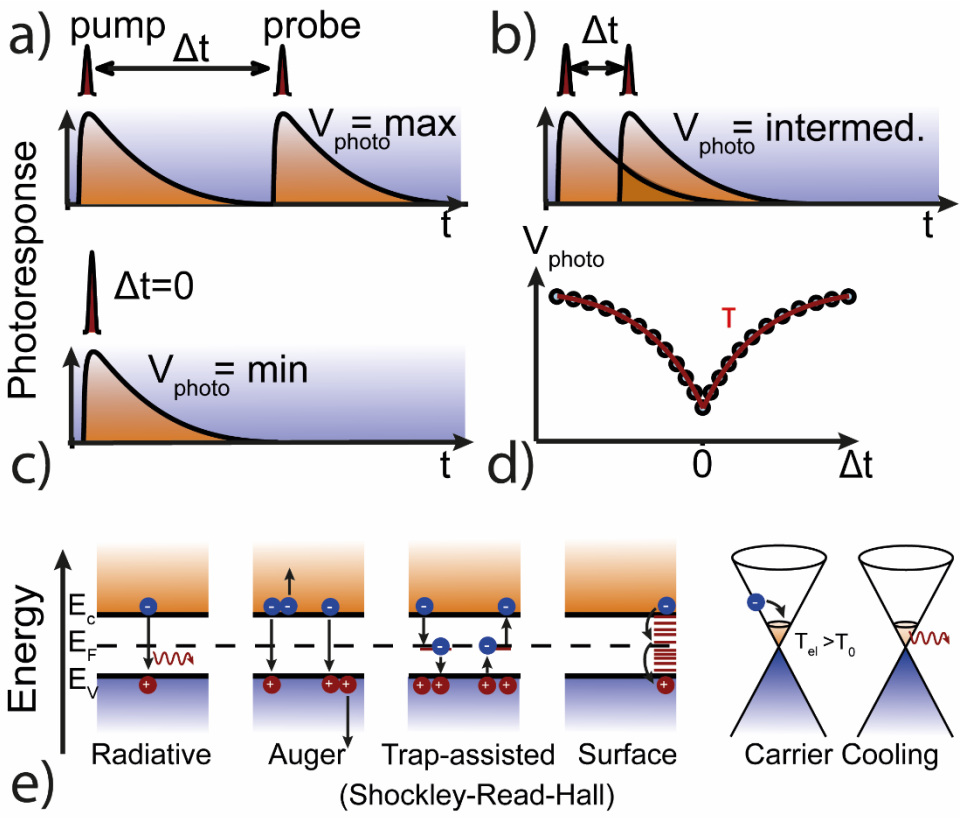

a-d) Adapted with permission from ref.[4] Copyright 2022 American Chemical Society.

Mono- vs. Multilayers

A key feature of most TMDCs is the direct-to-indirect bandgap transition upon crystal growth from a truly two-dimensional monolayer to multilayers.[16] Since direct optical transitions exhibit larger extinction coefficients and usually faster recombination times, it is generally assumed that TMDC monolayers are superior for photodetection in both, sensitivity and speed. Indeed, for the intrinsic photoresponse this holds true, as demonstrated e.g. for two terminal $MoTe_2$ photodetectors with thicknesses of 2 nm to 35 nm and response times of 4 ps to almost 1 ns, respectively (Figure 1).[17] In addition to the effect of the direct-to-indirect bandgap transition, this finding could be rationalized further in terms of the quantum mechanical wave function model,[18] predicting that bulk defects in $MoTe_2$ have a much longer lifetimes than surface defects, which increases the intrinsic response time.

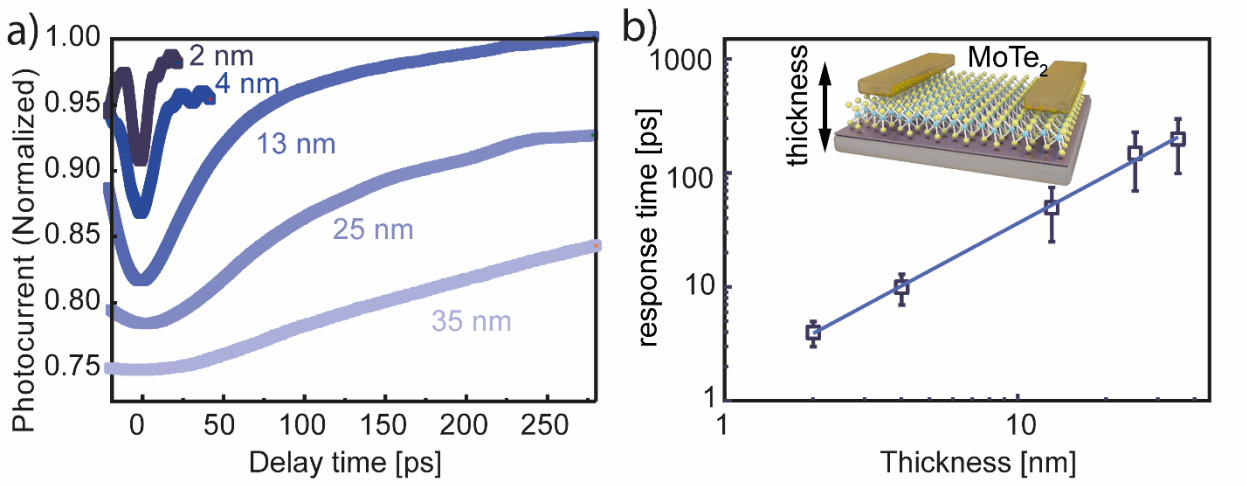

Figure 1. a) 2PC results in $MoTe_2$ two-terminal photodetectors showing longer intrinsic response times with increasing $MoTe_2$ thickness. (b) Thickness dependence of the intrinsic response time in $MoTe_2$ two-terminal photodetectors. Reproduced from ref.[17] Copyright 2022, Elsevier B.V.

For the extrinsic photoresponse however, additional factors must be considered, which may outcompete the intrinsic advantages of monolayers. These include the stronger total absorbance of

multilayers (due to longer optical path lengths) and the concomitant increase in photocurrent as well as material-specific differences in the lifetimes of surface defects. For MoS_2 for instance, monolayers exhibit three orders of magnitude longer extrinsic response times than multilayers of 10 nm thickness, presumably due to deep surface trap states, which become increasingly screened in the bulk.[19] This behavior is also often referred to as persistent photocurrent, a feature that is quite prominent in MoS_2 and severely limits the prospects of MoS_2 monolayers as fast photodetectors.[20]

For WSe_2 in contrast, we have recently shown that the extrinsic response time is much more robust against surface trap states.[1] Here, the major speed limitation is the RC time, which scales with the *photo*resistance of the devices. Monolayers of TMDCs exhibit less total absorbance and, thus, fewer photoexcited charge carriers which leads to longer RC times. In principle, this disadvantage can be addressed by increasing the irradiance as we will detail below.

Speed-limiting factors to the extrinsic photoresponse

The results and conclusions in this section are based on our work with two-terminal lateral photodetectors based on MoS_2 or WSe_2, which we use as a model device architecture due to its cost-effective fabrication. A key result of these studies is that such simple photodetectors are essentially all limited by the RC constant of the device. While this may not necessarily be true for more complicated TMDC photodetectors, such as gated three-terminal devices, vertical geometries or heterostructures, we believe that the considerations here should be widely applicable also to other TMDC materials within two-terminal lateral detectors. Therefore, this section focuses on strategies for decreasing the RC time, which are validated by monitoring the overall effect on the extrinsic photoresponse.

Substrate effects

To illustrate the importance of the substrate material on which the TMDC is deposited, we focus on the surface roughness and the dielectric constant. The substrate roughness is particularly relevant for TMDC monolayers as an uneven surface enhances carrier scattering. Moreover, since most carrier transport occurs in the few TMDC layers located closest to the electrodes, such carrier scattering also affects bulk TMDC crystals. We have measured bulk WSe_2 on (smooth) glass and (rough) polyimide substrates. Polyimide yields lower dark currents by more than two orders of magnitude, cf. Figure 2, presumably due to its rougher surface (30.7 ± 11.6 nm vs 5.5 ± 0.7 nm on glass). Such an increase in the resistance is detrimental to the RC time and the expected response time. In a similar context, Haizmann *et al.* have recently shown that substrate roughness and its effect on thin TMDC layers also alters the orientation of small molecules adsorbed to the TMDC surface.[21] While the exact consequences of this alteration remain to be explored, it is likely that this will affect the chemical interactions at the interface and, thus, the efficiency with which such small molecules saturate surface defects. Therefore, a popular and powerful strategy is the insertion of an atomically smooth protection layer of hexagonal boron nitride underneath the TMDC layer. This action improves the charge carrier mobility, however at the expense of additional fabrication steps.[22]

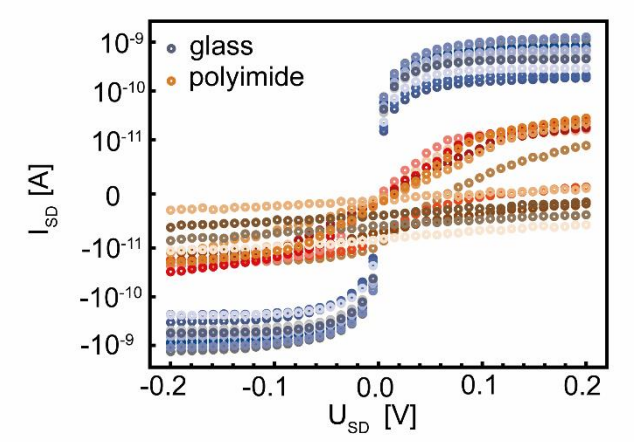

Figure 2. Dark currents of WSe_2 photodetectors on polyimide (orange) and glass (blue). Adapted from Ref.[3] with permission from the PCCP Owner Societies.

For bulk WSe_2, we found that the dielectric constant of the substrate not only alters the response time but also the speed-limiting mechanism. Glass has a larger dielectric constant of 4.5 – 8, in comparison to the weaker screening on polyimide with 3.7. For polyimide, the WSe_2 detectors are faster and limited by the RC time.[3] For the detectors on glass, the response time is slower than the RC constant, presumably now limited due to drift limitation as a consequence of a shrunken depletion layer induced by the higher dielectric screening (Figure 3). The maximal achieved bandwidth is 2.6 MHz.

In summary, the ideal substrate for fast photodetection is smooth and does not reduce the depletion zone below the channel width to avoid a drift-limited photoresponse. The latter can be avoided with low-k substrates, however at the cost of increased RC times.

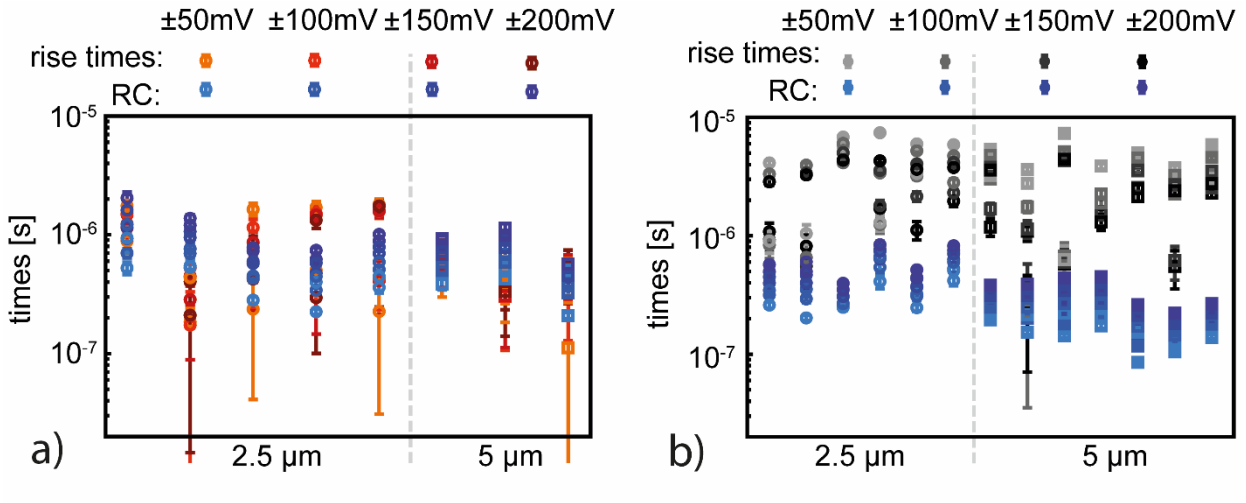

Figure 3. Measured rise times and calculated $R_{illum}C$-time on a) glass and b) polyimide substrates. The X-axes list all measured contacts with the respective channel length. Adapted from Ref.[3] with permission from the PCCP Owner Societies.

Influence of the electrical contact

Layered materials offer several ways of contacting: bottom electrodes beneath the TMDC, top electrodes above the material, and a sandwich structure in a vertical stack or so-called "edge contacts" at the edges of the material. A key result of our work with MoS_2 is that edge contacts provide unique advantages for the speed of photodetectors based on anisotropic 2D materials, such as TMDCs. With the unravelling of the edge, for example by plasma etching, there is direct access to the layers which differ chemically tremendously from the surface.[23] They have been shown to provide a lower contact resistance, a smaller transfer length or a higher capability of charge carrier injection.[22,24] We find that this contact style accelerates the fall time of the photodetectors by more than an order of magnitude (Figure 4).[2] This result is presumably the combination of three effects: First and foremost, by contacting the edge of the TMDC, access to the much higher in-plane mobility is given. No van-der-Waals gaps between layers have to be overcome, instead the excitons in the layers can be extracted in parallel and the interlayer transfer time is irrelevant for the photoresponse. Second, the work function of the MoS_2 on the edges is different than on the top facet, which affects the magnitude of a potential Schottky barrier at the TMDC/metal interface.[23] Both of these effects take specific advantage of the anisotropic in-plane/out-of-plane carrier behavior in TMDCs.

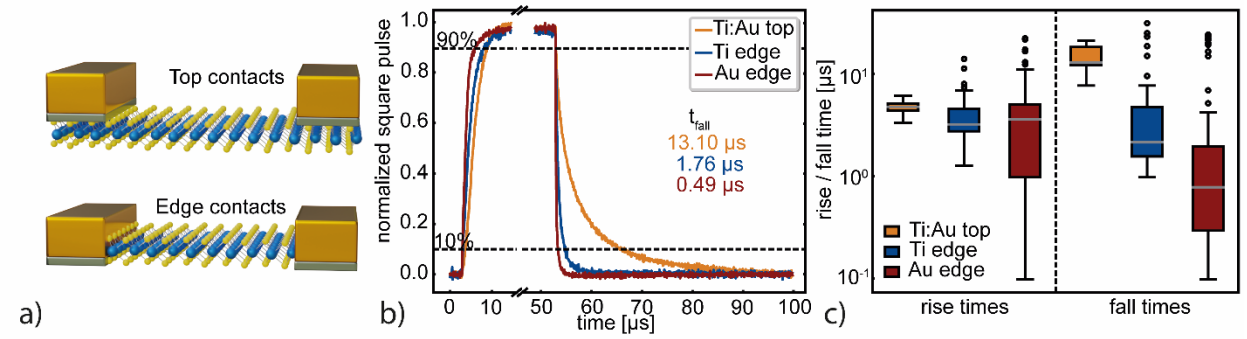

Figure 4. a) Scheme of a top contacted and edge contacted device. b) Normalized square pulse

response of a top contacted (ochre), a titanium edge contacted (blue), and a gold edge contacted device (red). c) box-and-whisker plots of all measurements showing rise and fall time for each electrode configuration. Adapted from Ref.[2] with permission from the Royal Society of Chemistry.

A third effect arises from the fact that top contacts often use adhesion layers, e.g. titanium, between the TMDC and the actual metal contact, e.g. gold. In the edge contact geometry, there is almost no contact between the TMDC and the adhesion layer, which again affects the height of a potential Schottky barrier at the interface. For the specific example of titanium vs. gold, we find that pure titanium edge contacts are faster than the top devices, but slower than Au edge devices. This is in agreement with Zhang et al. who correlated the faster response times for Au contacts with a higher Schottky barrier.[25]

All advantages of edge contacts combined lead to accelerated rise and fall times, also visible when comparing the non-steady state and Fourier transform. The representative example shown in Figure 5 displays an acceleration of more than 80x. The fastest device obtained in this study exceeded 18 MHz.

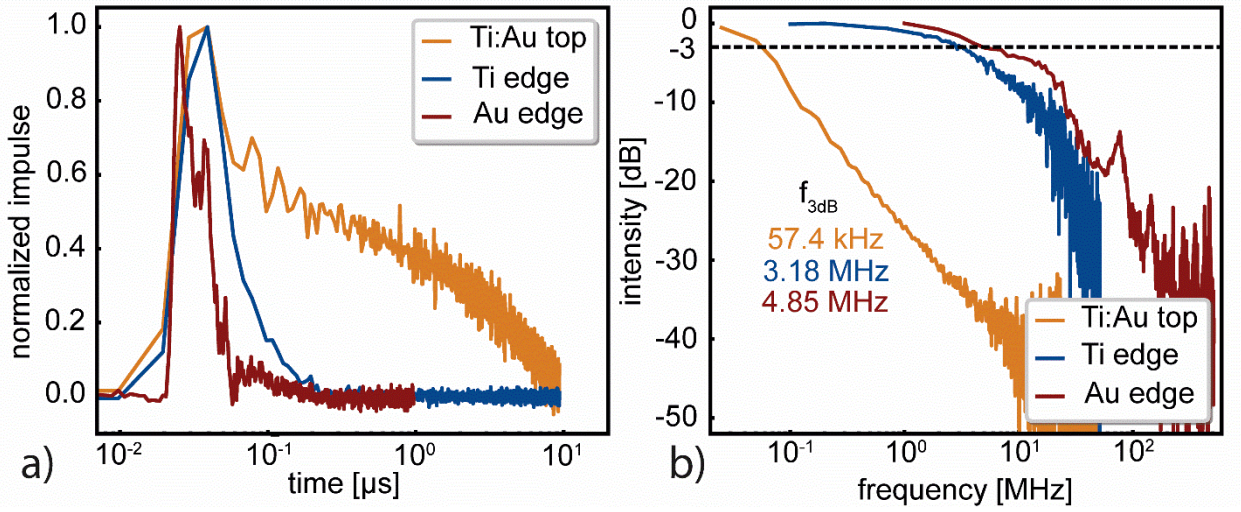

Figure 5. a) Normalized impulse response for the top and Ti edge device as well as for the Au

edge device. b) power spectrum of the impulse response in a). Adapted from Ref.[2] with permission from the Royal Society of Chemistry.

With respect to the widely applied top contact architectures in the design of TMDC photodetectors, we note an additional complication: these contacts are typically fabricated by thermal evaporation of the metal in vacuum. Hot metal atoms induce defects and alloy formation in the top layers of the TMDC, leading to Fermi-level pinning and other potentially unwanted changes to the surface with detrimental effects on the speed of the photodetector.[24] Several strategies have been designed to circumvent this complication, including transfer printing of metal electrodes via polymer stamps or so-called van-der-Waals electrodes.[26,27] Geladari et al. have recently shown that solutions of atom precise Au_{32}-metalloid gold clusters can be utilized as inks for direct laser-induced printing of gold contacts with diffraction-limited spatial resolution.[28] The clusters are separated and stabilized with ($nBuP_{12}Cl_8$) linkers. Upon illumination at 488 nm these linkers are detached from the Au cores, which then fully agglomerate to macroscopic, metallic gold. This way, gold contacts with near bulk-like conductivities (10^6 S/m) were defined on WS_2, and a fully functional photodetector was fabricated without thermal evaporation, cf. Figure 6. The thermal stress inflicted by such methods is only given by the absorption of light, which strongly limits the imposition on the WS_2 flake. While quantitative details remain to be fully investigated, we expect such gentle contacting strategies to be advantageous in reducing the carrier injection time, which would manifest in a reduced RC time.

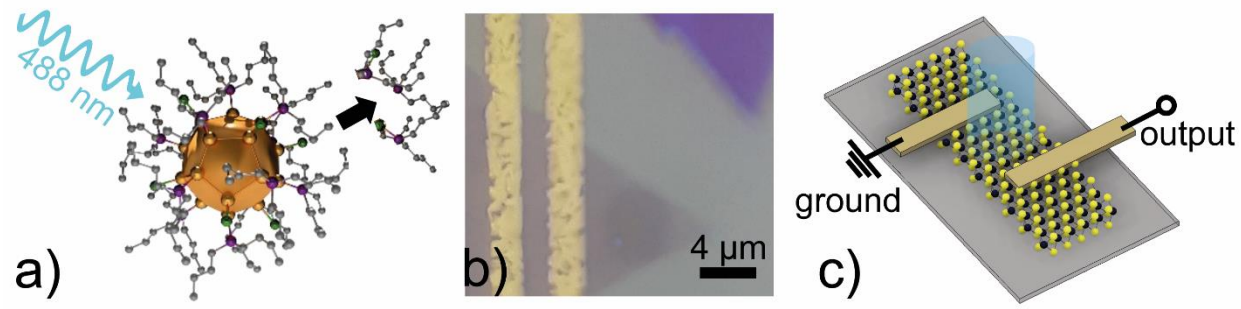

Figure 6. a) Schematic process of linker detachment upon laser illumination. b) Optical microscope image of exemplary electrodes and c) scheme of two electrode device. Adapted from Ref.[28] Copyright 2023, Wiley-VCH.

Reduction of the RC constant

An important observation from our work with TMDC photodetectors is that under typical optical excitation conditions (irradiance between 0.4 W/cm^2 and 400 W/cm^2), the photoactive material does not saturate. This means that larger irradiances – either due to higher laser power or better optical focusing – invoke lower photoresistance since additional charge carriers are excited. As the RC constant of a photodetector scales directly with the *photo*resistance (not the resistance in the dark), increasing the irradiance is a simple yet effective means for increasing the speed of TMDC photodetectors. This becomes apparent in Figure 7(a) which depicts the dependence of the response time in WSe_2 multilayers on the photoresistance, which is varied solely by changing the irradiance. The strong negative correlation indicates the aforementioned RC limitation, which is further verified by quantitative agreement with the calculated and fitted RC constants of the devices.[29]

Another effective means for decreasing the RC time is a reduction of the device dimensions, which lowers the resistance and capacitance simultaneously.[1] By reducing the channel width from 25 to 20 µm (80 µm in the previous studies with substrate effects[3]), the electrode width itself from 10 to 1 µm and the channel length from 2.5 to 1 µm, the capacitance is approximately reduced from 7.6 to 4 fF (24 fF previously[3]). For this example, we obtain a response time < 2 ns and a 3dB bandwidth of 230 MHz compared to roughly 30 MHz for the larger device geometry (Figure 7b). We note that this bandwidth is a conservative, lower-bound estimate, since such WSe_2 are so fast that they exceed the current speed limit of our set-up as verified with a commercial photodiode

with an expected bandwidth of 1.75 GHz as a reference (Figure 7b, orange line). Further reduction of the channel width and length to 1 µm or below are easily achieved with electron beam lithography, and we expect such future optimizations to result in 3dB bandwidths close to, if not beyond 1 GHz.

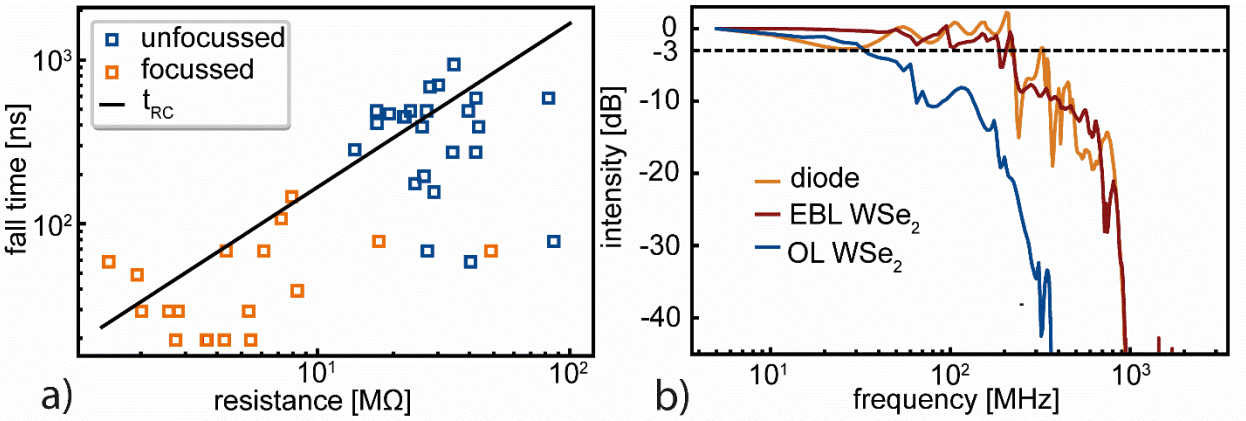

Figure 7. a) Fall time plotted against photoresistance for an optically lithographed WSe_2 flake. The measurements were performed with different irradiances between 0.4 and 400 W/cm^2. The black line is the estimated RC time of the device. b) Power spectrum of the impulse responses. Blue shows an optically lithographed flake, red the WSe_2 flake fabricated with the smaller geometry via electron beam lithography. Ochre shows a commercial photodiode with a nominal bandwidth of 1.75 GHz. Measurements of the diode and the EBL flake were made without transimpedance amplifier (bandwidth 175 MHz). Adapted from Ref.[1] with permission from the Royal Society of Chemistry.

In the context of energy-efficient optical communication, one may be concerned with the energy consumption of such a photodetector considering that the irradiance required for optimal speed of roughly 100 W/cm^2 is quite high. For our example and a bandwidth of (at least) 230 MHz, a laser power of 6.25 µW is sufficient. Since the detector is operated at zero bias by taking advantage of the photovoltaic voltage generated at the metal/semiconductor junction, the laser power is the only

significant contribution to the overall energy consumption, which amounts to < 27 fJ/bit. This compares favorably to most optical communication components (>1000 fJ/bit) and is not much higher than the energy required to switch a simple CMOS gate (~1 fJ/bit).[30]

Exploring and expanding the ultimate speed limit for TMDC photodetectors

With the strategies detailed above in place, one may expect to finally lift the current RC limitation of two-terminal TMDC photodetectors. Ultimately, and under the assumption that drift as well as diffusion times remain insignificant, the speed limit of such optimized devices will be determined by their intrinsic material response times. Assessing and optimizing these is therefore relevant in determining materials and architectures that provide the highest prospects for true GHz performance in optical applications. For example, 2PC measurements of an MoS_2 monolayer in a two-terminal photodetector with a simple metal-semiconductor-metal configuration without external bias has revealed an intrinsic response with a fast component of 3-5 ps and a slow component of 80-100 ps.[31] This picosecond response is derived from defect-related recombination processes. Upon photoexcitation, the thermalization and cooling of excited carriers occurs on the time scale of 0.5-1 ps. After that, these charge carriers are captured by different defects such as surface defects and grain boundaries with different lifetimes, which determine the intrinsic speed limit of the photodetector.

2PC measurements of the intrinsic response time may also be used to explore the potential of more complicated TMDC device structures, such as vertical van der Waals p-n junction heterostructures. The strong built-in electric field in these junctions has been shown to greatly reduce the carrier drift time. This mitigates the detrimental effect of thick multilayers (see the example of $MoTe_2$ in Figure 1) and allows exploiting the larger total absorbance of bulk crystals. An example is the MoS_2/25 nm WSe_2 heterostructure depicted in Figure 8 which in addition to the

built-in field takes advantage of type-II band alignment to separate the charge carriers. With 8.9 ps, the intrinsic response in the heterostructure is 50 times faster than in the pure 25 nm WSe_2 two terminal photodetectors with 426 ps.[32]

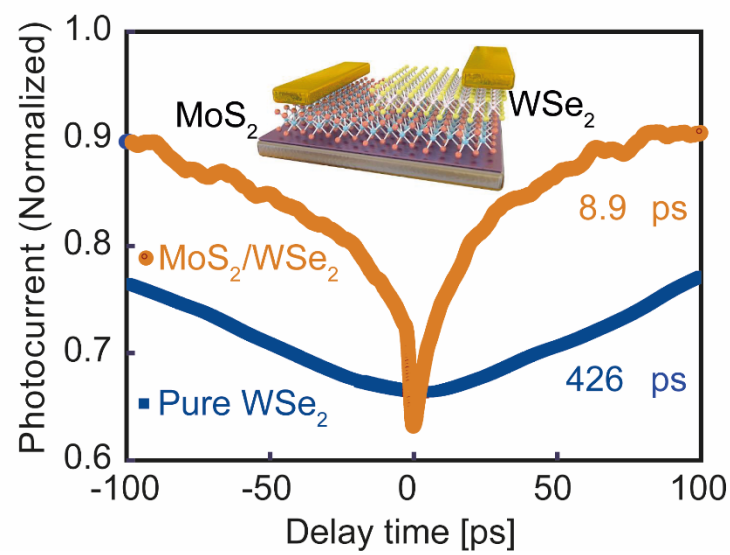

Figure 8. Comparison of the intrinsic response time in a pure 25 nm WSe_2 two-terminal photodetector with a MoS_2/25 nm WSe_2 p-n junction. Reproduced from ref.[32] Copyright 2022, Wiley-VCH.

Heterostructures with ultrafast intrinsic response times may also be used to design TMDC-based photodetectors for operation in the infrared region. With pure TMDCs, this is challenging due to their large bandgaps, especially when targeting the important telecommunication band at 1560 nm. For the conventional photo-thermoelectric effect, hot carriers in TMDCs need to relax through phonon-mediated cooling, where the energy of the hot carriers is transported to the lattice and the lattice temperature can be considered equal to that of the carriers, resulting in a slow response time. This restriction may be lifted by integrating graphene into the TMDC photodetector. In this configuration, the low-energy photon-induced hot carriers from graphene can be injected into the TMDC and the spectral window of the TMDC photodetector is broadened.[33] The generated charge

carriers in graphene can relax via carrier-carrier scattering without the assistance of the lattice. For pure graphene, this advantage becomes apparent in terms of an intrinsic response time of 1.5 ps at room temperature.[34] However, pure graphene exhibits high dark currents and, thus, low detectivities. Combining graphene with WS_2 to a van-der-Waals heterostructure preserves the ultrafast hot carrier cooling and results in a response time of 1.2 ps under 1560 nm excitation (Figure 9). This photodetector combines the advantage of the low dark current in TMDCs and the fast hot carrier cooling as well as infrared sensitivity of graphene. If the extrinsic limits of these devices could be lifted at least to some extent, these ultrafast intrinsic response times suggest that GHz device operation should be easily feasible with TMDCs, even in the infrared regime.

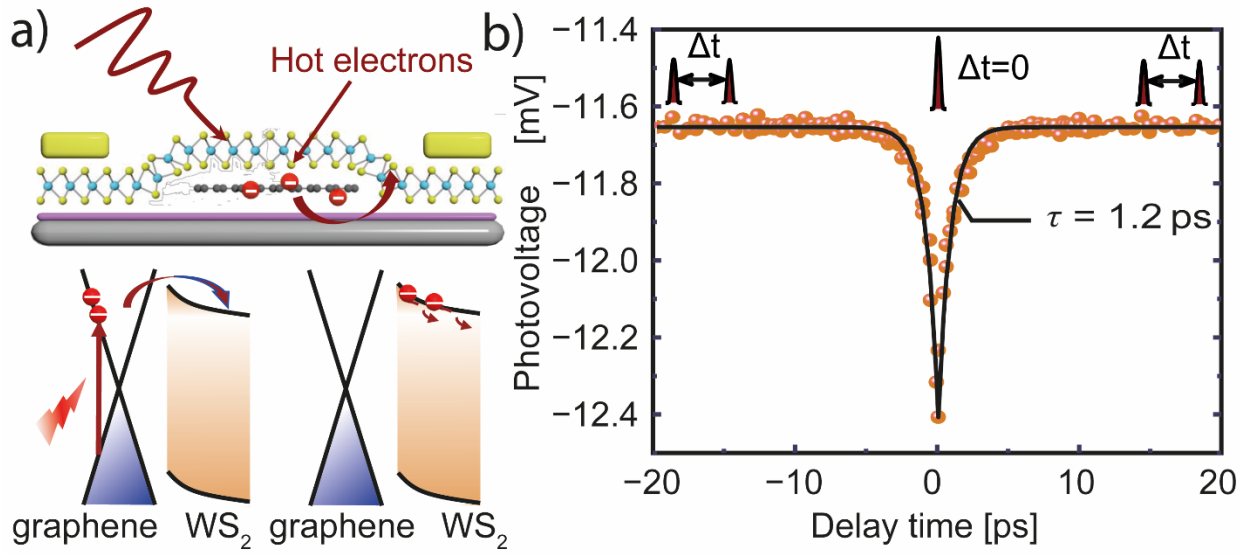

Figure 9. a) Schematic illustration of the WS_2/graphene photodetector for harvesting low energy photons. b) Intrinsic response time of a WS_2/graphene photodetector at 270 K with 1560 nm excitation.

Outlook

We conclude this account with a short outlook on promising future strategies to reduce the current gap in TMDC photodetectors between extrinsic response times of ~ 2 ns and the ultrafast intrinsic response of < 2 ps.

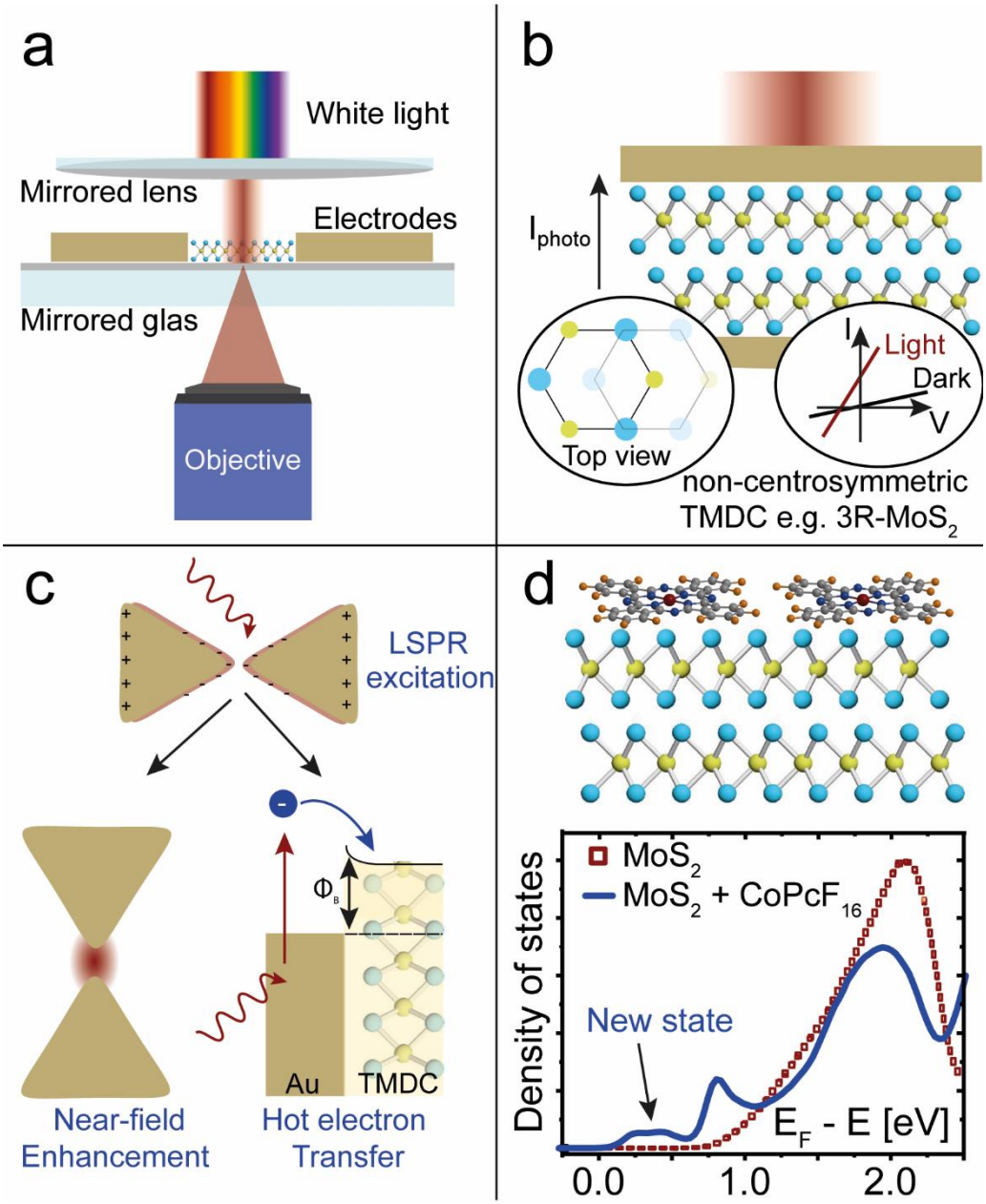

Figure 10. a) Scheme of a modified Fabry-Pérot resonator with a contacted TMDC photodetector inside. b) Sketch of a vertical photodetector with 3R-MoS_2 for harvesting the bulk photovoltaic

effect. c) Near field enhancement and hot electron transfer of a plasmonic structure following excitation of the localized surface plasmon. d) The adsorption of perfluorinated cobalt phthalocyanine onto bulk n-type MoS_2 lowers the Fermi level and induces a gap state at the interface.

Optical cavities

Implementing a photodetector into an optical cavity, e.g. a Fabry-Pérot resonator, leads to a confinement of the electromagnetic field[35] and an alteration of the emission rate of the photoactive material.[36] By tuning the length of the cavity, optical transitions in resonance with a cavity mode are selectively amplified (Figure 10a).[36] This coupling can have several advantageous effects for fast photodetection, such as the tuning of the lifetime of the photoexcited state or an increased carrier mobility. The latter has been demonstrated for a perylene diimide derivative and resulted in an increase of one order of magnitude, presumably due to a polariton-mediated delocalization of excitons.[37] For the coupling to be strong, it is important that the reabsorption of emitted photons is efficiently possible, which favors materials with small Stokes shifts, such as WS_2.[38] One can expect that strong coupling between photodetector and optical cavity will drastically enhance the speed and efficiency of the device, which is the basis for the emerging field of polaritonic chemistry.[39]

Bulk Photovoltaic Effect

Conventional photodetectors are subject to a trade-off between speed and responsivity.[8] In photoconductive devices it is desirable for the responsivity to create gain via long lifetimes of the minority carriers, but this action simultaneously invokes long response times. Here, the so-called bulk photovoltaic effect (BPVE) can be advantageous, which is a nonlinear optical process that occurs in non-centrosymmetric materials, creating an anomalous current. It takes advantage of

spontaneous electronic polarization to separate charge carriers to result in theoretically high photoelectric conversion efficiencies.[40] Potential candidates for its exploitation are the rhombohedral 3R-phase of many TMDCs that naturally possess an out-of-plane polarization (Figure 10b) or heterostructures where the required breaking of the inversion symmetry is created at the interface. In a graphene/3R-MoS_2/graphene heterostructure, this concept demonstrated an intrinsic response time of 2 ps,[41] indicating a high photodetection bandwidth comparable to graphene.[34] Moreover, the conversion efficiency for the BPVE is related to the free path length (l_0), which refers to the non-thermalized carrier transit length before they descend to the bottom of the conductive band.[40] Due to the small thickness of the graphene/3R-MoS_2/graphene heterostructure, the vertical charge carrier collection distance is smaller than l_0, resulting in a responsivity of 70 mA/W^{-1} and EQE of 16 %, which is large considering the fast speed of the detector.[42]

Plasmonics

Another approach to simultaneously enhance the speed and responsivity of photodetectors is the coupling to localized surface plasmon resonances (LSPR).[43] A localized surface plasmon is the collective oscillation of the free electron gas within a metallic nanostructure, which decays on the timescale of picoseconds after excitation.[44,44] The radiative component of this decay plays a key role in the near-field enhancement of the electric field, while the non-radiative component generates hot electrons (Figure 10c). The resonances, decay components and -times can be tuned by the chemical nature and morphology of the nanostructure, e.g. with sharp structures like stars.[45,46] A fast collection of the hot electrons provided, plasmonic/TMDC detectors exhibit bandwidths in the GHz regime.[47,48] The simultaneous near-field enhancement of plasmonic structures is advantageous for the responsivity, and an 1000-fold increases in photocurrent as well as the extension of the spectral range has been demonstrated for a Pt-plasmonic/MoS_2

photodetector.[49] The combination of ultrafast hot electrons, high near field enhancements, potential use of plasmonic lattices and the extended detection range hold great promise to reach tens of GHz bandwidths with good responsivities in TMDCs.[50]

Chemical defect engineering by molecular adlayers

TMDCs exhibit a large propensity for surface defects, e.g. due to volatile chalcogens or adsorbates introduced during device fabrication, which lead to undesirable trap states and doping. If these trap states are located deep within the band gap (as for instance in MoS_2), the resulting long lifetimes of the trapped carriers greatly decrease the speed of the photodetector. A promising strategy to mitigate this inherent disadvantage of 2D-materials is the formation of van-der-Waals heterostructures employing molecular adlayers, such as metal phthalocyanines. Haizmann *et al.* have shown by angle-resolved photoelectron spectroscopy that the adsorption of perfluorinated cobalt-phthalocyanine ($CoPcF_{16}$) on bulk n-type MoS_2 restores an intrinsic position of the Fermi level, indicating that trap states near the conduction band edge could be compensated by the adlayer.[51] This action was accompanied by the appearance of a new gap state near the Fermi level, which was strongly confined to the interface (Figure 10d). In contrast, the fluorine-free analogue CoPc did not induce a new gap state but increased the degree of n-doping in the heterostructure. This highlights that molecular adlayers allow for chemical control over surface defects in TMDCs, rendering them an important tool for future improvements of the (defect-sensitive) speed of TMDC photodetectors toward the GHz range.

Conclusion

The speed of simple two-terminal photodetectors based on TMDC mono- or multilayers is mostly RC limited. We have shown in a series of papers that relatively facile means are sufficient to accelerate their extrinsic response time to < 2 ns, which enables near-GHz photodetection. These

means include the choice of the substrate, a reduction of the device dimensions, the design of the contacts as well as diffraction-limited optics. Insights from intrinsic photoresponse measurements suggest that further improvements are feasible, but these will most likely require new concepts, especially when focusing on maximizing the gain-bandwidth product. These concepts include the saturation of defects by molecular adlayers, the replacement of thermally evaporated metal contacts by printed electrodes, the combination of TMDCs with optical cavities or plasmonic nanostructures as well as the exploitation of the bulk photovoltaic effect.

AUTHOR INFORMATION

Corresponding Author

* Marcus Scheele; marcus.scheele@uni-tuebingen.de

Author Contributions

The manuscript was written through contributions of all authors. All authors have given approval to the final version of the manuscript.

ACKNOWLEDGMENT

Financial support of this work has been provided by the Deutsche Forschungsgemeinschaft (DFG) under grant SCHE1905/9-1 (project no. 426008387) as well as the European Research Council (ERC) under the European Union's Horizon 2020 research and innovation program (grant agreement No 802822).

REFERENCES

(1) Strauß, F.; Kohlschreiber P.; Keck, J.; Michel, P. M.; Hiller, J.; Meixner, A. J.; Scheele, M. A Simple 230 MHz Photodetector Based on Exfoliated WSe_2 Multilayers. *ChemRxiv Preprint* **2023**. https://doi.org/10.26434/chemrxiv-2023-0lmgq

(2) Strauß, F.; Schedel, C.; Scheele, M. Edge Contacts Accelerate the Response of MoS_2 Photodetectors. *Nanoscale Adv.* **2023**, 3494–3499.

(3) Schedel, C.; Strauß, F.; Kohlschreiber, P.; Geladari, O.; Meixner, A. J.; Scheele, M. Substrate Effects on the Speed Limiting Factor of WSe_2 Photodetectors. *Phys. Chem. Chem. Phys.* **2022**, *24*, 25383–25390.

(4) Maier, A.; Strauß, F.; Kohlschreiber, P.; Schedel, C.; Braun, K.; Scheele, M. Sub-Nanosecond Intrinsic Response Time of PbS Nanocrystal IR-Photodetectors. *Nano Lett.* **2022**, *22*, 2809–2816.

(5) Chernikov, A.; Berkelbach, T. C.; Hill, H. M.; Rigosi, A.; Li, Y.; Aslan, O. B.; Reichman, D. R.; Hybertsen, M. S.; Heinz, T. F. Exciton Binding Energy and Nonhydrogenic Rydberg Series in Monolayer WS_2. *Phys. Rev. Lett.* **2014**, *113*, 076802.

(6) Bernardi, M.; Palummo, M.; Grossman, J. C. Extraordinary Sunlight Absorption and One Nanometer Thick Photovoltaics Using Two-Dimensional Monolayer Materials. *Nano Lett.* **2013**, *13*, 3664–3670.

(7) Pang, C. S.; Zhou, R.; Liu, X.; Wu, P.; Hung, T. Y. T.; Guo, S.; Zaghloul, M. E.; Krylyuk, S.; Davydov, A. V.; Appenzeller, J.; Chen, Z. Mobility Extraction in 2D Transition Metal Dichalcogenide Devices—Avoiding Contact Resistance Implicated Overestimation. *Small* **2021**, *17*, 2100940.

(8) Sorger, V. J.; Maiti, R. Roadmap for Gain-Bandwidth-Product Enhanced Photodetectors: Opinion. *Opt. Mater. Express* **2020**, *10*, 2192.

(9) Wadhwa, R.; Agrawal, A. V.; Kumar, M. A Strategic Review of Recent Progress, Prospects and Challenges of MoS_2-Based Photodetectors. *J. Phys. D: Appl. Phys.* **2022**, *55*, 063002.

(10) Huo, N.; Konstantatos, G. Recent Progress and Future Prospects of 2D-Based Photodetectors. *Adv. Mater.* **2018**, *30*, 1801164.

(11) Zhang, Y.; Ma, K.; Zhao, C.; Hong, W.; Nie, C.; Qiu, Z. J.; Wang, S. An Ultrafast WSe_2 Photodiode Based on a Lateral p-i-n Homojunction. *ACS Nano* **2021**, *15*, 4405–4415.

(12) Gould, M.; Baehr-Jones, T.; Ding, R.; Hochberg, M. Bandwidth Enhancement of Waveguide-Coupled Photodetectors with Inductive Gain Peaking. *Opt. Express* **2012**, *20*, 7101–7111.

(13) Schedel, C.; Strauß, F.; Scheele, M. Pitfalls in Determining the Electrical Bandwidth of Nonideal Nanomaterials for Photodetection. *J. Phys. Chem. C* **2022**, *126*, 14011–14016.

(14) Razeghi, M.; Rogalski, A. Semiconductor Ultraviolet Detectors. *J. Appl. Phys.* **1996**, *79*, 7433–7473.

(15) Zeng, Z.; Wang, Y.; Pan, A.; Wang, X. Ultrafast Photocurrent Detection in Low-Dimensional Materials. *Phys. Status Solidi Rapid Res. Lett.* **2023**, *18*, 2300120.

(16) Cheiwchanchamnangij, T.; Lambrecht, W. R. L. Quasiparticle Band Structure Calculation of Monolayer, Bilayer, and Bulk MoS_2. *Phys. Rev. B Condens. Matter Mater. Phys.* **2012**, *85*, 205302.

(17) Zeng, Z.; Braun, K.; Ge, C.; Eberle, M.; Zhu, C.; Sun, X.; Yang, X.; Yi, J.; Liang, D.; Wang, Y.; Huang, L.; Luo, Z.; Li, D.; Pan, A.; Wang, X. Picosecond Electrical Response in Graphene/$MoTe_2$ Heterojunction with High Responsivity in the near Infrared Region. *Fundam. Res.* **2022**, *2*, 405–411.

(18) Wang, H.; Zhang, C.; Rana, F. Surface Recombination Limited Lifetimes of Photoexcited Carriers in Few-Layer Transition Metal Dichalcogenide MoS_2. *Nano Lett.* **2015**, *15*, 8204–8210.

(19) Tang, W.; Liu, C.; Wang, L.; Chen, X.; Luo, M.; Guo, W.; Wang, S. W.; Lu, W. MoS_2 Nanosheet Photodetectors with Ultrafast Response. *Appl. Phys. Lett.* **2017**, *111*, 153502.

(20) Chandan; Sarkar, S.; Angadi, B. Defects Induced Persistent Photoconductivity in Monolayer MoS_2. *Appl. Phys. Lett.* **2021**, *118*, 172105.

(21) Haizmann, P.; Juriatti, E.; Klein, M.; Greulich, K.; Nagel, P.; Merz, M.; Schuppler, S.; Ghiami, A.; Ovsyannikov, R.; Giangrisostomi, E.; Chassé, T.; Scheele, M.; Peisert, H.; Nano, K.; Facility, M. Orientation of Cobalt-Phthalocyanines on Molybdenum Disulfide: Distinguishing between Single Crystals and Small Flakes. *J. Phys. Chem. C* **2024**. https://doi.org/10.1021/acs.jpcc.3c06707

(22) Jain, A.; Szabó, Á.; Parzefall, M.; Bonvin, E.; Taniguchi, T.; Watanabe, K.; Bharadwaj, P.; Luisier, M.; Novotny, L. One-Dimensional Edge Contacts to a Monolayer Semiconductor. *Nano Lett.* **2019**, *19*, 6914–6923.

(23) Asadi, M.; Kumar, B.; Behranginia, A.; Rosen, B. A.; Baskin, A.; Repnin, N.; Pisasale, D.; Phillips, P.; Zhu, W.; Haasch, R.; Klie, R. F.; Král, P.; Abiade, J.; Salehi-Khojin, A. Robust Carbon Dioxide Reduction on Molybdenum Disulphide Edges. *Nat. Comm.* **2014**, *5*, 4470.

(24) Allain, A.; Kang, J.; Banerjee, K.; Kis, A. Electrical Contacts to Two-Dimensional Semiconductors. *Nat. Mater.* **2015**, *14*, 1195–1205.

(25) Zhang, W.; Chiu, M. H.; Chen, C. H.; Chen, W.; Li, L. J.; Wee, A. T. S. Role of Metal Contacts in High-Performance Phototransistors Based on WSe_2 Monolayers. *ACS Nano* **2014**, *8*, 8653–8661.

(26) Jin, K.; Li, T.; Cai, H.; Li, M.; Pan, N.; Wang, X. Transfer Printing of Metal Electrodes for High Performance InSe Photodetectors. *Opt Commun.* **2019**, *436*, 47–51.

(27) Zhao, Q.; Jie, W.; Wang, T.; Castellanos-Gomez, A.; Frisenda, R. InSe Schottky Diodes Based on Van Der Waals Contacts. *Adv. Funct. Mater.* **2020**, *30*, 2001307.

(28) Geladari, O.; Eberle, M.; Maier, A.; Fetzer, F.; Chassé, T.; Meixner, A. J.; Scheele, M.; Schnepf, A.; Braun, K. Nanometer Sized Direct Laser-Induced Gold Printing for Precise 2D-Electronic Device Fabrication. *Small Methods* **2023**, *7*, 2201221.

(29) Nabetl, B.; Lioul, L.; Paolella, A. Transit Time and RC Time Constant Trade-Offs in MSM Photodetectors. *IEEE Princeton Section Sarnoff Symposium.* **1993**, 187–191.

(30) Miller, D. A. B. Attojoule Optoelectronics for Low-Energy Information Processing and Communications. *J. Light. Technol.* **2017**, *35*, 346–396.

(31) Wang, H.; Zhang, C.; Chan, W.; Tiwari, S.; Rana, F. Ultrafast Response of Monolayer Molybdenum Disulfide Photodetectors. *Nat. Comm.* **2015**, *6*, 8831.

(32) Zeng, Z.; Ge, C.; Braun, K.; Eberle, M.; Wang, Y.; Zheng, B.; Zhu, C.; Sun, X.; Huang, L.; Luo, Z.; Chen, Y.; Duan, H.; Wang, S.; Li, D.; Gao, F.; Pan, A.; Wang, X. Manipulating Picosecond Photoresponse in van Der Waals Heterostructure Photodetectors. *Adv. Funct. Mater.* **2022**, *32*, 2200973.

(33) Wang, W.; Klots, A.; Prasai, D.; Yang, Y.; Bolotin, K. I.; Valentine, J. Hot Electron-Based Near-Infrared Photodetection Using Bilayer MoS_2. *Nano Lett.* **2015**, *15*, 7440–7444.

(34) Sun, D.; Aivazian, G.; Jones, A. M.; Ross, J. S.; Yao, W.; Cobden, D.; Xu, X. Ultrafast Hot-Carrier-Dominated Photocurrent in Graphene. *Nat. Nanotechnol.* **2012**, *7*, 114–118.

(35) Konrad, A.; Metzger, M.; Kern, A. M.; Brecht, M.; Meixner, A. J. Controlling the Dynamics of Förster Resonance Energy Transfer inside a Tunable Sub-Wavelength Fabry-Pérot-Resonator. *Nanoscale* **2015**, *7*, 10204–10209.

(36) Purcell, E. M. Spontaneous Emission Probabilities at Radio Frequencies. In *Confined Electrons and Photons: New Physics and Applications*; Burstein, E., Weisbuch, C., Eds.; Springer US: Boston, MA, 1995; p 839.

(37) Orgiu, E.; George, J.; Hutchison, J. A.; Devaux, E.; Dayen, J. F.; Doudin, B.; Stellacci, F.; Genet, C.; Schachenmayer, J.; Genes, C.; Pupillo, G.; Samorì, P.; Ebbesen, T. W. Conductivity in Organic Semiconductors Hybridized with the Vacuum Field. *Nat. Mater.* **2015**, *14*, 1123–1129.

(38) Niehues, I.; Marauhn, P.; Deilmann, T.; Wigger, D.; Schmidt, R.; Arora, A.; Michaelis De Vasconcellos, S.; Rohlfing, M.; Bratschitsch, R. Strain Tuning of the Stokes Shift in Atomically Thin Semiconductors. *Nanoscale* **2020**, *12*, 20786–20796.

(39) Baranov, D. G.; Wersäll, M.; Cuadra, J.; Antosiewicz, T. J.; Shegai, T. Novel Nanostructures and Materials for Strong Light-Matter Interactions. *ACS Photonics* **2018**, *5*, 24–42.

(40) Spanier, J. E.; Fridkin, V. M.; Rappe, A. M.; Akbashev, A. R.; Polemi, A.; Qi, Y.; Gu, Z.; Young, S. M.; Hawley, C. J.; Imbrenda, D.; Xiao, G.; Bennett-Jackson, A. L.; Johnson, C. L. Power Conversion Efficiency Exceeding the Shockley-Queisser Limit in a Ferroelectric Insulator. *Nat. Photonics* **2016**, *10*, 611–616.

(41) Wu, J.; Yang, D.; Liang, J.; Werner, M.; Ostroumov, E.; Xiao, Y.; Watanabe, K.; Taniguchi, T.; Dadap, J. I.; Jones, D.; Ye, Z. Ultrafast Response of Spontaneous Photovoltaic Effect in 3R-MoS_2-Based Heterostructures. *Science Adv.* **2022**, *8*, 3759.

(42) Yang, D.; Wu, J.; Zhou, B. T.; Liang, J.; Ideue, T.; Siu, T.; Awan, K. M.; Watanabe, K.; Taniguchi, T.; Iwasa, Y.; Franz, M.; Ye, Z. Spontaneous-Polarization-Induced Photovoltaic Effect in Rhombohedrally Stacked MoS_2. *Nat. Photonics* **2022**, *16*, 469–474.

(43) Brongersma, M. L.; Shalaev, V. M. The Case for Plasmonics. *Science* **2010**, *328*, 440–441.

(44) Steiner, A. M.; Lissel, F.; Fery, A.; Lauth, J.; Scheele, M. Prospects of Coupled Organic–Inorganic Nanostructures for Charge and Energy Transfer Applications. *Angew. Chem. Int. Ed.* **2021**, *60*, 1152–1175.

(45) Besteiro, L. V.; Yu, P.; Wang, Z.; Holleitner, A. W.; Hartland, G. V.; Wiederrecht, G. P.; Govorov, A. O. The Fast and the Furious: Ultrafast Hot Electrons in Plasmonic Metastructures. Size and Structure Matter. *Nano Today* **2019**, *27*, 120–145.

(46) Zhu, Y.; Xu, H.; Yu, P.; Wang, Z. Engineering Plasmonic Hot Carrier Dynamics toward Efficient Photodetection. *Appl. Phys. Rev.* **2021**, *8*, 021305.

(47) Li, Z.; Hu, S.; Zhang, Q.; Tian, R.; Gu, L.; Zhu, Y.; Yuan, Q.; Yi, R.; Li, C.; Liu, Y.; Hao, Y.; Gan, X.; Zhao, J. Telecom-Band Waveguide-Integrated MoS_2 Photodetector Assisted by Hot Electrons. *ACS Photonics* **2022**, *9*, 282–289.

(48) Flöry, N.; Ma, P.; Salamin, Y.; Emboras, A.; Taniguchi, T.; Watanabe, K.; Leuthold, J.; Novotny, L. Waveguide-Integrated van Der Waals Heterostructure Photodetector at Telecom Wavelengths with High Speed and High Responsivity. *Nat. Nanotechnol.* **2020**, *15*, 118–124.

(49) Kumar, R.; Sharma, A.; Kaur, M.; Husale, S. Pt-Nanostrip-Enabled Plasmonically Enhanced Broad Spectral Photodetection in Bilayer MoS_2. *Adv. Opt. Mater.* **2017**, *5*, 1700009.

(50) Dorodnyy, A.; Salamin, Y.; Ma, P.; Plestina, J. V.; Lassaline, N.; Mikulik, D.; Romero-Gomez, P.; Morral, A. F. I.; Leuthold, J. Plasmonic Photodetectors. *IEEE J. Sel. Top. Quantum Electron.* **2018**, *24*, 1–13.

(51) Haizmann, P.; Juriatti, E.; Klein, M.; Greulich, K.; Ovsyannikov, R.; Giangrisostomi, E.; Chassé, T.; Peisert, H.; Scheele, M. Tuning the Interfacial Electronic Structure of MoS_2 by Adsorption of Cobalt Phthalocyanine Derivatives. *ChemRxiv Preprint* **2023**. https://doi.org/10.26434/chemrxiv-2024-4kc0h.

TOC graphic:

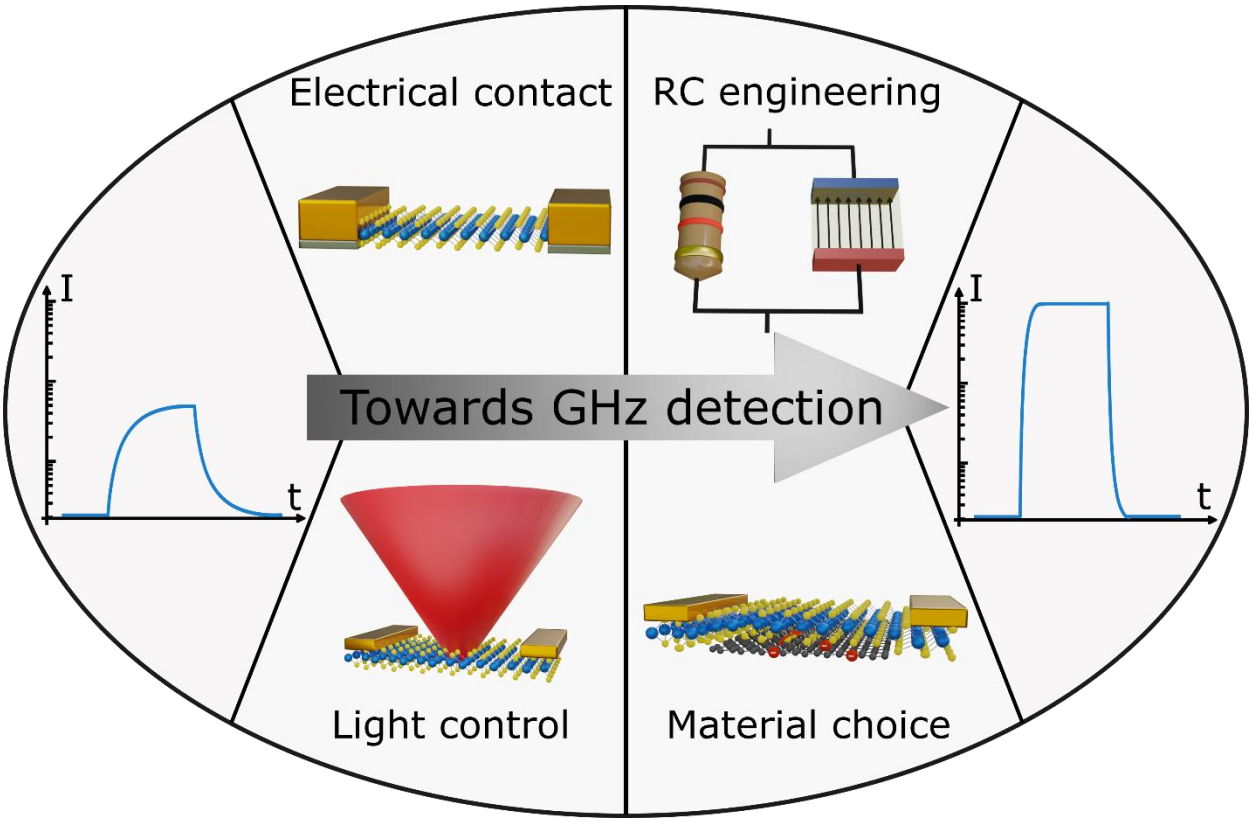

Textcount:

Author names + Title: 14 words

Text (Introduction – Author Information): 4967 words

Total: = 4981 words